NASA/TM—2009-215508

Measurement of Trap Length for an Optical Trap

Susan Y. Wrbanek
Glenn Research Center, Cleveland, Ohio

May 2009

NASA STI Program . . . in Profile

Since its founding, NASA has been dedicated to the advancement of aeronautics and space science. The NASA Scientific and Technical Information (STI) program plays a key part in helping NASA maintain this important role.

The NASA STI Program operates under the auspices of the Agency Chief Information Officer. It collects, organizes, provides for archiving, and disseminates NASA's STI. The NASA STI program provides access to the NASA Aeronautics and Space Database and its public interface, the NASA Technical Reports Server, thus providing one of the largest collections of aeronautical and space science STI in the world. Results are published in both non-NASA channels and by NASA in the NASA STI Report Series, which includes the following report types:

- TECHNICAL PUBLICATION. Reports of completed research or a major significant phase of research that present the results of NASA programs and include extensive data or theoretical analysis. Includes compilations of significant scientific and technical data and information deemed to be of continuing reference value. NASA counterpart of peer-reviewed formal professional papers but has less stringent limitations on manuscript length and extent of graphic presentations.

- TECHNICAL MEMORANDUM. Scientific and technical findings that are preliminary or of specialized interest, e.g., quick release reports, working papers, and bibliographies that contain minimal annotation. Does not contain extensive analysis.

- CONTRACTOR REPORT. Scientific and technical findings by NASA-sponsored contractors and grantees.

- CONFERENCE PUBLICATION. Collected papers from scientific and technical conferences, symposia, seminars, or other meetings sponsored or cosponsored by NASA.

- SPECIAL PUBLICATION. Scientific, technical, or historical information from NASA programs, projects, and missions, often concerned with subjects having substantial public interest.

- TECHNICAL TRANSLATION. English-language translations of foreign scientific and technical material pertinent to NASA's mission.

Specialized services also include creating custom thesauri, building customized databases, organizing and publishing research results.

For more information about the NASA STI program, see the following:

- Access the NASA STI program home page at *http://www.sti.nasa.gov*

- E-mail your question via the Internet to *help@sti.nasa.gov*

- Fax your question to the NASA STI Help Desk at 301–621–0134

- Telephone the NASA STI Help Desk at 301–621–0390

- Write to:
  NASA Center for AeroSpace Information (CASI)
  7115 Standard Drive
  Hanover, MD 21076–1320

NASA/TM—2009-215508

Measurement of Trap Length for an Optical Trap

Susan Y. Wrbanek
Glenn Research Center, Cleveland, Ohio

National Aeronautics and
Space Administration

Glenn Research Center
Cleveland, Ohio 44135

May 2009

This report is a formal draft or working paper, intended to solicit comments and ideas from a technical peer group.

This report contains preliminary findings, subject to revision as analysis proceeds.

This work was sponsored by the Fundamental Aeronautics Program at the NASA Glenn Research Center.

Level of Review: This material has been technically reviewed by technical management.

Available from

NASA Center for Aerospace Information
7115 Standard Drive
Hanover, MD 21076–1320

National Technical Information Service
5285 Port Royal Road
Springfield, VA 22161

Available electronically at http://gltrs.grc.nasa.gov

Measurement of Trap Length for an Optical Trap

Susan Y. Wrbanek
National Aeronautics and Space Administration
Glenn Research Center
Cleveland, Ohio 44135

Abstract

The trap length along the beam axis for an optical trap formed with an upright, oil-immersion microscope was measured. The goals for this effort were twofold. It was deemed useful to understand the depth to which an optical trap can reach for purposes of developing a tool to assist in the fabrication of miniature devices. Additionally, it was desired to know whether the measured trap length favored one or the other of two competing theories to model an optical trap. The approach was to trap a microsphere of known size and mass and raise it from its initial trap position. The microsphere was then dropped by blocking the laser beam for a pre-determined amount of time. Dropping the microsphere in a free-fall mode from various heights relative to the coverslip provides an estimate of how the trapping length changes with depth in water in a sample chamber on a microscope slide. While it was not possible to measure the trap length with sufficient precision to support any particular theory of optical trap formation, it was possible to find regions where the presence of physical boundaries influenced optical traps, and determine that the trap length, for the apparatus studied, is between 6 and 7 μm. These results allow more precise control using optical micromanipulation to assemble miniature devices by providing information about the distance over which an optical trap is effective.

Introduction

NASA has a need to use novel new micro and nanoscale materials to fabricate miniature flight sensors in order to unobtrusively measure conditions inside engines for its fundamental aeronautics program (Refs. 1 to 4). Newly developed nanotube clusters were identified as material that can be used to assemble such an unobtrusive sensor (Refs. 5 to 8). Optical trapping and optical micromanipulation techniques are being investigated to assess their usefulness as an assembly tool for miniature flight sensors.

Optical micromanipulation presents a clear advantage over other micromanipulation techniques such as atomic force microscopy (AFM) or "self assembly" in the case where material can be "grown" in the desired location. An optical trap can lift and manipulate material of interest without dragging it across a substrate as must happen with AFM. Also, because there is no mechanical contact between the optical trap and objects under manipulation, mechanical damage to the microscopic material will not occur (Ref. 9). Additionally, it will likely be necessary to position microscopic material in locations where material cannot be grown onto another surface. For these reasons, optical micromanipulation is under development as a tool to manipulate and position microscopic material to make the advanced, unobtrusive flight sensors of the future. Also, optical trapping and micromanipulation can aid in sample handling in remote, humanly inaccessible locations in support for the Vision for Space Exploration.

While several reports exist concerning the measurement of the strength of an optical trap, (Refs. 10 to 14) no information has been found by this author concerning the longitudinal (direction of beam propagation) distance that an optical trap is effective. In 1985 Arthur Ashkin reported the first single-beam gradient force optical trap with which he was able to trap dielectric particles. He reported the existence of a "backward force," (Ref. 11) that drew polystyrene microspheres upward toward the focus of a downward-propagating, tightly-focused laser beam. Previous to that experiment, Ashkin had reported optical trapping in terms of the results of two forces, the gradient force (F_{grad}) which pushes dielectric material along the intensity gradient of the beam toward the center, and the scattering force (F_{scatt}) which

pushes the particles in the direction of beam propagation. In experiments previous to his 1985 work, Ashkin had only observed particles moving toward the center of the beam, and along the direction of propagation, unless the net force in the direction of propagation was balanced by an equal force oppositely directed (Ref. 15).

In order to use optical trapping for placement of dielectric particles in relation to a substrate or other material of interest, understanding the distance over which an optical trap is effective in the direction of propagation of the beam is essential. This knowledge is particularly helpful in the case where microscopic particles must be lifted up, carried over to and deposited onto a substrate. Additionally, it is useful to know if the effective trapping length of an optical trap remains the same everywhere inside the sample chamber, or if the trap length is location dependent. Knowledge of the distance over which an optical trap is effective for a particular optical tweezers apparatus will aid in determining procedures for assembling miniature sensor devices.

Experiment

The effective trapping length of the optical tweezers beam can be calculated using a time-of-flight technique. If a falling microsphere is falling at its terminal velocity, the weight of the microsphere is balanced by the buoyant force and the drag force supplied by the water, thus the velocity is constant. For a falling minute particle in a sufficiently viscous medium, the terminal velocity can be reached in a distance that is short compared to the radius of the particle (Ref. 16). Then, by measuring the time a sphere is allowed to fall from a fixed optical trap, and noting whether or not the particle can be retrapped, one can compute the effective trap length. The maximum distance from the trap center that a microsphere can be retrapped can be determined by dropping the microsphere and allowing it to fall for successively longer time intervals.

In order to proceed with determining the effective length of the optical trap (d), the terminal velocity (V_T) and time of fall of the microsphere (t) needed to be determined.

$$d = V_T \times t \tag{1}$$

The optical tweezers beam was prepared for these measurements by slightly overfilling a NA (numerical aperture) = 1.25, 100x oil immersion microscope objective lens with a collimated 25 mW beam from a 532 nm Neodymium- Vandadate ($Nd:YVO_4$) Gaussian laser. The direction of beam propagation at the optical trap was downward. The microscope's focus was adjusted by adjusting the height of the sample stage, while the objective lens remained fixed. The microscope was equipped with indicators on the fine focus knob that allowed the change in height of the objective lens to be measured in micrometers. The indicators on the focus knob of the microscope compared very well to other laboratory measuring devices for over 1 cm of travel, and deemed to be reliable and repeatable. This was particularly true when all motion was in one direction, thus avoiding potential backlash in the knob adjustment. The sample particles were prepared by sealing 9.975±0.061 μm diameter polystyrene (PST) microspheres in water between a glass microscope slide and coverslip. The 9.975 μm diameter microspheres were chosen because they were the only microspheres available at that time that did not contain any noticeable electrostatic charge. A schematic of the experimental setup is shown in Figure 1. An enlarged diagram of the sample chamber is shown in Figure 2.

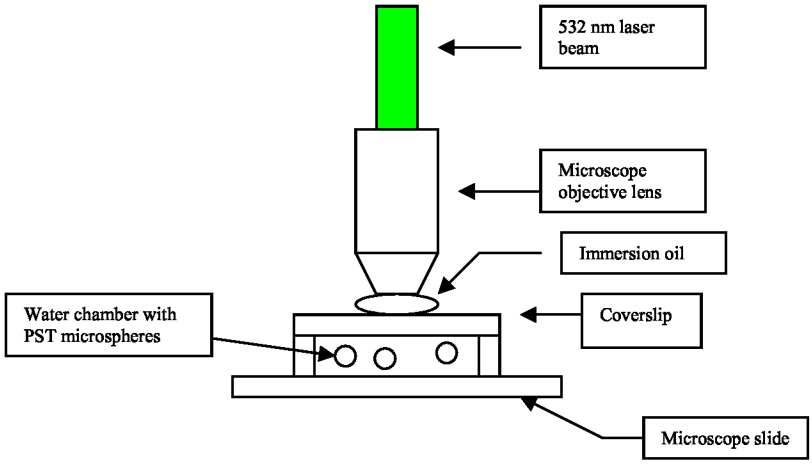

Figure 1.—Illustration showing the relationship to the optical trapping beam and the water chamber containing the sample. The diagram is not to scale.

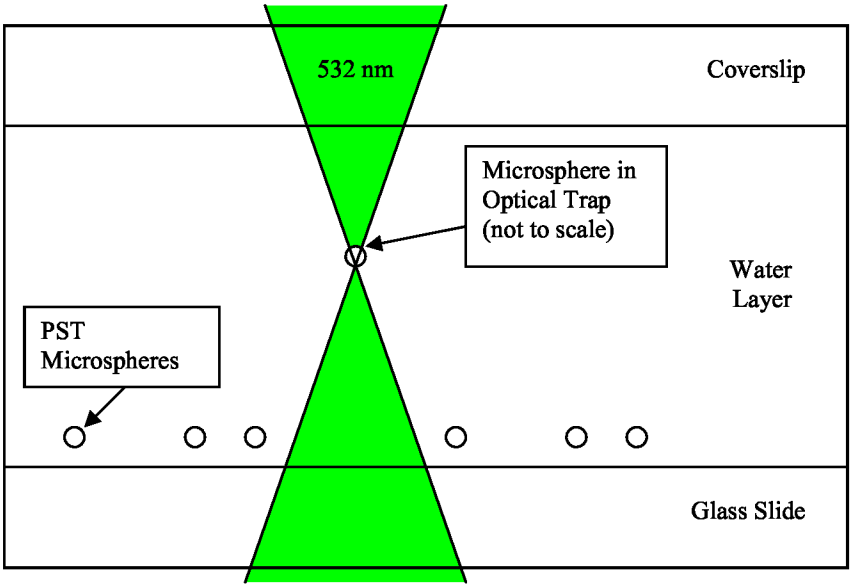

Figure 2.—Schematic showing the sample chamber cross section. The water layer between the glass slide and coverslip contains PST microspheres that were raised in an optical trap and subsequently dropped to determine water layer height, the spheres' terminal velocity, and the trapping length. The sample chamber is illuminated by an incandescent light for locating the PST microspheres with microscope. The diagram is not to scale.

Water Chamber Height Measurements

In order to know the height of the coverslip and the distance through which the sphere may fall it was necessary to know the height of the sample layer on the microscope slide.

The depth of the sample chamber was measured in two ways. In the first method, the microscope slide and coverslip thicknesses were measured separately with a micrometer. Then the completely assembled slide was measured, and the thicknesses of the slide and coverslip subtracted from the total. Using these micrometer measurements, the height of the water layer was determined to be 122.8±3.4 μm.

In the second method, ink marks were placed on the bottom of the coverslip and the top of the microscope slide before the package was assembled. Then the focus positions of the two marks were noted using a 40x and 10x objectives with a laboratory microscope. This method yielded results that were nearly in agreement with the micrometer measurements when shorter focal length objectives such as the 40x objective on the microscope were used. The water chamber depth obtained by this method ranged from 131.1±3.3 to 139.7±3.9 μm. Repeating the microscope measurements with the 10x objective resulted in some good agreement about the depth of the sample chamber however, not always. The depths recorded using the 10x objective ranged from 119.1±8.5 to 143.2±5.9 μm. The uncertainty is much larger for the 10x objective as the depth of focus is greater than that for a higher power objective, resulting in greater uncertainty of the focus position.

There appears to be greater variance measuring the chamber thickness using the microscope with any objective than with the micrometer, because it is necessary for the observer to move one's head to read the height, and then return to looking through the microscope to focus on the next ink mark. It is unlikely that one's eyes are repositioned the same distance from the microscope eyepiece, thus there is greater scatter in the measurements made with this method. Other magnifications, such as the use of a 60x objective were not available on the microscope that was used. Measuring the thickness using a 100x objective was tried, but it could not be positioned sufficiently close to the top of the slide to focus on that ink mark due to the presence of the coverslip. Placing a camera on the microscope could eliminate the difficulty of trying to replace one's head with respect to the eyepiece after each change is made, but such a camera was not available at the time the measurements were made.

A third method of determining water chamber depth that was attempted was to use a time-of-flight method. It was also planned to optically trap a 9.975 diameter polystyrene microsphere against the underside of the coverslip, note the microscope stage height and then allow the microsphere to fall the bottom of the sample chamber. By moving the stage to keep the microsphere in focus, and noting the height change of the stage and the time the microsphere took to fall, it was hoped to determine the height of the water layer. However, it was not possible to distinguish when the microsphere had actually settled on the microscope slide, resulting in unreasonable fall times. This method was rejected in determining the water layer height.

Terminal Velocity Measurements

In order to determine the velocity with which a microsphere fell from a trapped position and was retrapped, several experiments were performed. First, a microsphere was optically trapped and raised in the sample chamber until it just touched the coverslip. The trap was then lowered a short distance from the coverslip. The trapping beam was blocked and the microsphere was then allowed to fall for a pre-determined period of time. The initial trap position caused the microsphere to appear slightly out of focus, apparently above the focus of the objective lens. When the microsphere fell through a position where the sphere was in focus, the timer was started and the fine focus was adjusted in order to follow the sphere as it fell. At the end of a specified time, the trapping beam was restored which caught the microsphere. Simultaneously the timer was halted, and the height of the microscope stage was again noted. Thus, the time and distance from the upper position when the sphere appeared in focus to the lower trapping point could be noted. Polystyrene microspheres were allowed to fall for periods of about 5, 10, 15, 20, and 30 sec. From this information an average velocity from the upper focus to the lower focus could be

obtained. The average velocity of the particle was found to be nearly constant regardless of the time interval for which the sphere fell. This supports the assertion that the terminal velocity for the PST microsphere was apparently reached very soon after its release from the optical trap.

The velocity of the falling spheres found via this method ranged from 2.7 to 3.8 μm/s, with an average of about 3.3 μm/s. It was found, that in general, the longer the microscope illumination light remained on, the faster the microspheres appeared to fall. A discussion of the effects of temperature of the fluid on the terminal velocity of a falling microsphere will be discussed later. There was no appreciable difference in the velocity determined from short or long time intervals.

Calculation of Terminal Velocity

According to Stokes Law, as a small spherical body with a small velocity moves through a fluid, the sphere is subjected to a force $\mathbf{F_s}$ such that, for a sphere of radius r, and velocity $\mathbf{v}$:

$$\mathbf{F_s} = -6\pi\eta r\mathbf{v} \tag{2}$$

where η is the viscosity of the fluid, r is the radius of the sphere and $\mathbf{v}$ is the velocity of the sphere. The sum of the vertical forces on the sphere can be represented as:

$$\Sigma\mathbf{F_y} = \mathbf{F_w} - \mathbf{F_B} - \mathbf{F_s} = m\mathbf{a} \tag{3}$$

where $\mathbf{F_w}$ is the weight of the sphere, $\mathbf{F_B}$ is the buoyant force on the sphere. When terminal velocity is reached, the forces balance and the acceleration is zero. The terminal velocity $\mathbf{V_T}$ can then be calculated as:

$$\mathbf{V_T} = (\mathbf{F_w} - \mathbf{F_B})/-6\pi\eta r \tag{4}$$

Calculating the terminal velocity for a falling 4.9875 μm radius PST microsphere, assuming the water remains at room temperature, results in a terminal velocity of 2.7 μm/s. The measured velocities in the previous section are in good agreement with this prediction.

However, it was noted that the slide and its contents are warmed by both the light source that illuminates the sample on the microscope as well as the trapping laser beam. An ANSI type E thermocouple was positioned on the opposite side of the sample microscope slide from the incident trapping laser beam (the same side as the incident scene illumination light, provided by an incandescent lamp). The temperatures there ranged from about 20 to 34 °C over the course of an hour's time manipulating PST microspheres. This has the effect of changing the water viscosity to give a calculated terminal velocity between 2.8 and 4.1 μm/s, as shown in Figure 3. Therefore the measured velocity range of 2.7 to 3.8 μm/s is in very good agreement with the predicted terminal velocity when the temperature of the water is taken into account.

The sample illumination light on the microscope was found to contribute more to the temperature of the water in the sample chamber than the laser did. This was probably because the laser was only on for a few seconds at a time, and then blocked. However the sample illumination light remained on for most of the day, contributing significantly to the warming of the sample chamber, and thus resulting in faster velocities late in each day's data collection. Future measurements may benefit from measuring the temperature at both the top and bottom exterior surfaces of the sample chamber, in order to better estimate the temperature of the water inside.

The trap length can then be determined by keeping the optical trap in a fixed position and dropping the microsphere with increasing time intervals. The maximum distance that the microsphere can travel and still be retrapped should be the trap length. Since there was little variation in the average velocities obtained previously, using a correct determination of the terminal velocity should provide a value from which the trapping length can be calculated. The uniformity in average velocities when the microsphere is dropped for successively longer time intervals indicates that the correct trap length determination is dependent on using the correct terminal velocity for the temperature of the sample and the measured time the microsphere fell before the trap was restored.

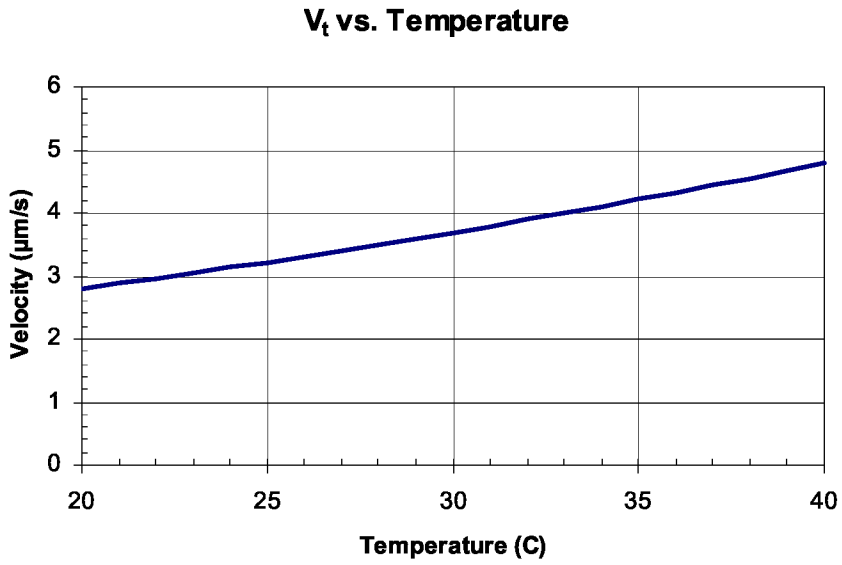

Figure 3.—Plot of calculated terminal velocity versus water temperature for a falling 9.975 µm diameter PST sphere in water, using Stokes equation.

Trapping Length Measurements

The distance along the z-axis, below the focus of the beam from which a particle can be trapped was also measured. This was done by trapping a particle and releasing it from several predetermined distances from the coverslip. The location of the coverslip was noted by trapping a 9.975 µm diameter polystyrene microsphere and raising the sphere in optical trap until the sphere just started to roll away along the coverslip. The microsphere in the optical trap was then quickly lowered a predetermined distance from the coverslip. A shutter was closed to block the beam allowing the microsphere to fall and at the same time a stopwatch was started. The stopwatch was stopped and the shutter opened as close to a predetermined time interval later as reaction time allowed. Noting whether the falling microsphere was drawn back up into the trap or not for successively longer falling times allowed computation of the distance through which the sphere fell, assuming it fell at a constant terminal velocity. This procedure was repeated for various starting distances from the coverslip.

The previous set of measurements demonstrated that each sphere reached its terminal velocity very quickly after being released, therefore multiplying the terminal velocity for a 9.975 µm diameter polystyrene microsphere by the average time interval measured yields a determination of the trapping length along the z-axis of the beam. As previously shown, it was necessary to monitor the temperature of the slide because prolonged exposure of the sealed slide to the light from the illumination source as well as the trapping beam increased the temperature locally on the slide. As noted above most of the heat was due to the illumination source.

From these measurements, the trapping length appeared to be affected by the distance of the sphere from the coverslip when it was released. When released closer to the coverslip more time, and possibly a longer distance, was available to retrap the sphere. If terminal velocity is reached almost immediately after beginning its fall, as has been shown earlier, then the trapping distance is longer near the coverslip. When the microsphere was lowered 4 or 5 µm from the position where it began to roll along the coverslip, retrapping the same sphere without changing the focus position of the objective lens was possible for 8 or 9 sec. Using terminal velocities found from Equations (2) to (4) it was found that a microsphere can still be retrapped after falling through a distance of 6 or 7 µm to a depth of about 30 µm from the coverslip. Closer to the coverslip, the trapping length appears to lengthen to nearly 24 µm, assuming that the sphere begins to fall when the beam is blocked.

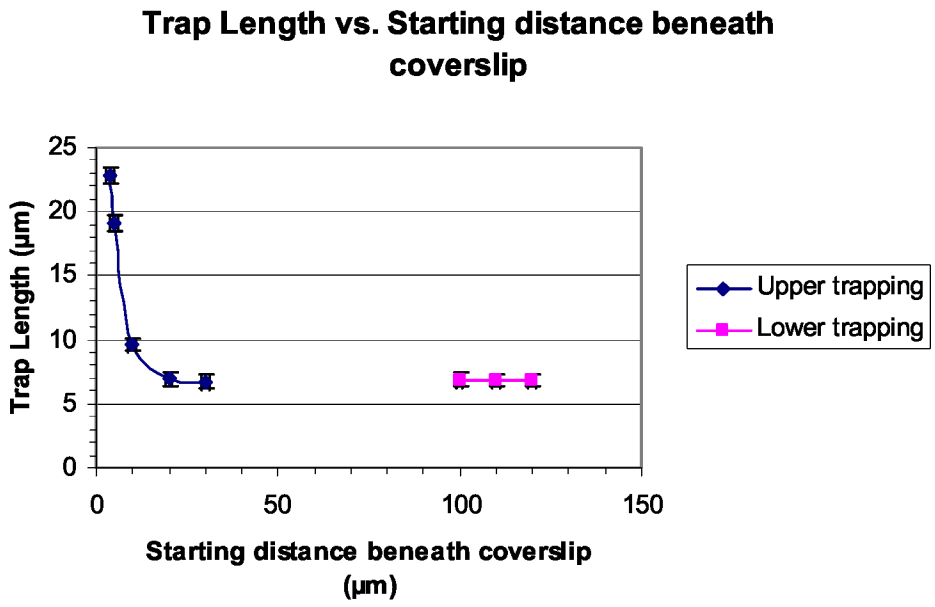

Figure 4.—Plot showing the trap length versus distance from coverslip for 100 percent retrap rates. Note that there are no 100 percent retrap rates at depths below 30 µm until 100 µm below the coverslip. Lines are included to guide the eye.

Figure 4 shows a plot of the trap length versus distance from the coverslip for starting distances where a successful retrap was accomplished 100 percent of the time. Each point represents an average of 10 drop and catch attempts. Near the middle of the sample chamber, at distances between 30 and 100 µm, the microsphere was not retrapped each time it was released, in that region successful retrapping was less than 100 percent. Note that the distance measurement is not to the center of the sphere, rather that it is the measured change of the sphere height after the sphere was brought to the coverslip.

Lock et al. (Ref. 18) state two predictions for trap length, depending on the model used to describe the trap beam. When the trap is modeled as a tightly focused Gaussian beam a trap length of ~6.9 µm is predicted, based on a calculation of position for which the computed radiation trapping force is directed upward (Ref. 18). However, when the beam is modeled as an Apertured, Focused, and Aberrated (AFA) beam, the trapping length is reduced to about 6.38 µm (Ref. 18). Since the terminal velocity obtained using Stokes equation does not provide enough precision to suggest which, if either, theory is a better predictor of trap length, it is useful to seek a modification to Stokes equation that suits the geometry of the sample cell when predicting terminal velocity for use in determining the actual trapping length of the optical trap.

Modifications of Stokes Equation

A modified version of Stokes equation is used by Wright et al. (Ref. 19) in 1994 describing the force on a sphere near a single wall. The modification is considered to be applicable because a no-slip boundary condition at the coverslip should increase the drag. This modified version of Stokes equation is described as:

$$F_s = \frac{6\pi r v \eta}{1 - \frac{9}{16}\left(\frac{r}{h}\right) + \frac{1}{8}\left(\frac{r}{h}\right)^3 - \frac{45}{256}\left(\frac{r}{h}\right)^4 - \frac{1}{16}\left(\frac{r}{h}\right)^5} \tag{5}$$

where v is the velocity of the particle, η is the viscosity of the fluid, r the radius of the particle, and h is described by Wright et al. to be the distance of the center of the sphere from the coverslip. If the determination of trap length using terminal velocities calculated by substituting the modified version of Stokes equation for the ordinary form of Stokes equation, then the velocities of the falling particles are considerably slower near the coverslip, shortening the trap lengths to be from nearly 23 μm to about 15 μm when the center of the microsphere is about 9 μm below the coverslip. However, Happel and Brenner (Ref. 20) report that the modification of Stokes equation used by Wright et al. to be valid for a particle falling parallel to a single wall. No mention is made as to whether that modification of Stokes equation applies to the top surface of a small enclosure. Happel and Brenner do report a different modification of Stokes equation for a particle moving toward a floor, but offer no advice as to what should be applied in the vicinity of ceilings.

The modification cited by Happel and Brenner for a particle moving toward a fixed wall results in Stokes law appearing as:

$$F = 6\pi\eta v a\lambda \tag{6}$$

Where η represents the viscosity of the fluid, v represents the velocity of the particle, and λ represents an infinite series described as:

$$\lambda = \frac{4}{3}\sinh\alpha\sum_{n=1}^{\infty}\frac{n(n+1)}{(2n-1)(2n+3)}\left[\frac{2\sinh(2n+1)\alpha+(2n+1)\sinh 2\alpha}{4\sinh^2(n+\frac{1}{2})\alpha-(2n+1)^2\sinh^2\alpha}-1\right] \tag{7}$$

and α is described as $\alpha = \cosh^{-1}(h/r)$, where h is the distance from the fixed wall to the center of the sphere, and r is the radius of the sphere.

Using this modification of Stokes equation in place of the original equation yields velocities that are slower still than those that result from the previous modification to Stokes equation. However, these velocities yield trapping lengths that are reduced to nearly 10 μm when the center of the microsphere is less than 15 μm away from the coverslip. A plot of trap length versus release distance from the coverslip can be found in Figure 5 showing the trap length as calculated with terminal velocities found using (1) Stokes equation (2) a modification to Stokes equation for motion parallel to a single wall; and (3) a modification to Stokes equation for motion toward a fixed wall. When the release distance from the coverslip is > 20 μm, all three equations yield very close results, as is expected when the distance of the falling sphere from container boundaries is sufficiently larger than the radius of the sphere to allow the modified versions of Stokes equation to approach the original version.

Uncertainty in timing the falling microspheres prevented the ability to distinguish via this method which beam model correctly predicts the trapping length for this optical tweezers system. The uncertainty in timing led to uncertainties in the trapping length that were typically about 0.35 to nearly 1 μm, neglecting uncertainties in temperature and distance measurements. Attempting to also consider temperature and distance uncertainties is not expected to improve the uncertainties in determination of the trap length at this time. However, one of the desired purposes of this experiment has been achieved, which is to be able to predict the distance over which this optical tweezers apparatus can draw microscopic objects upward into the trap. For purposes of using this optical tweezers apparatus to move and characterize microscopic material, it can now be said that the trap length is between 6 and 7 μm at most locations within the sample chamber.

Closer than 15 μm to the coverslip, the time available to retrap a microsphere could be longer than 7 sec, resulting in trap lengths that appeared to be 10 to 23 μm, depending on the version of Stokes equation used to compute the terminal velocity. Interactions between the microsphere and the coverslip, and the initial set-up of the flow of fluid around the sphere as it begins to move are not well enough understood at this time, to properly account for the increased time available to retrap a microsphere near the coverslip.

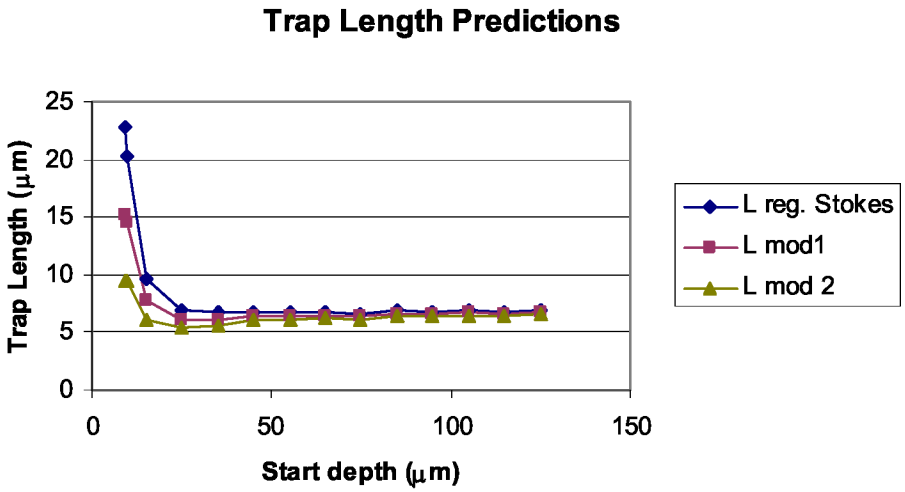

Figure 5.—Plot of trap length versus starting depth for the center of the microsphere, using temperature corrected terminal velocities computed using three different forms of Stokes equation. Lines have been included to better illustrate which points belong to each modification.

Measurement of Microsphere Retrapping Success Rate

Physical contact between the microsphere and the coverslip may produce sticking between the surfaces, delaying the fall of the microsphere. Attempts to measure the time allowable for a sphere to be retrapped when the microsphere was known to be in contact with the coverslip resulted in the microsphere sticking to the coverslip for 20 sec or more until it was dislodged by tapping on the microscope slide with a pencil. Further than 30 μm from the coverslip the microsphere could not be retrapped at all after about 2 sec until a depth of about 100 μm was reached. From a 100 to a 120 μm depth, a microsphere could be retrapped after about 2 sec but not for a longer time. From the previous measurements of the water layer height in the sample chamber, it is estimated that this region is between 20 and 30 μm from the bottom of the water layer of the sample chamber.

Several trials of trapping for increasing amounts of time were run at increasing distances from the coverslip, and the results are shown in Figures 6 and 7. The fraction of efforts for which a falling microsphere was successfully retrapped after a pre-determined amount of time was recorded.

Figure 6 plots percentage of successful retraps for 2 and 3-sec falling intervals starting at various distances below the coverslip. For falling intervals of 2 sec, the microspheres are easily retrapped after release lowering them 30 μm or less below the coverslip, and for distances between 100 and 120 μm below the coverslip. It is noted that for a 2-sec time interval successful retrapping occurred closer to the top and bottom boundaries of the sample chamber. While retrapping was not fully successful in the middle area of the chamber, the retrap percentage remained above 70 percent. Difficulty in retrapping a microsphere near the middle may in part be due to the sensitivity of the falling microsphere to subtle vibrations in the equipment that can cause the falling sphere to move horizontally away from the path of the optical trap.

Not only did the trap length decrease with depth in the water, but also the success rate of retrapping diminished with distance. As the drop point of the microsphere was lowered the number of tries for an average time that successful retrapping occurred decreased. For average dropping times of 2 sec the retrapping success rate began to decrease 40 μm below the coverslip to about 83 percent of the attempts. A 100 percent success rate of retraps was again achieved 100 μm below the coverslip. For an average dropping time of 3 sec the successful retrap rate declined to about 40 percent when the sphere began its fall 20 μm below the coverslip and never improved with depth. Figure 7, charts A, B, C, and D, show the percentage of time that a trapped microsphere was successfully retrapped for given distances the sphere was lowered from the top before releasing.

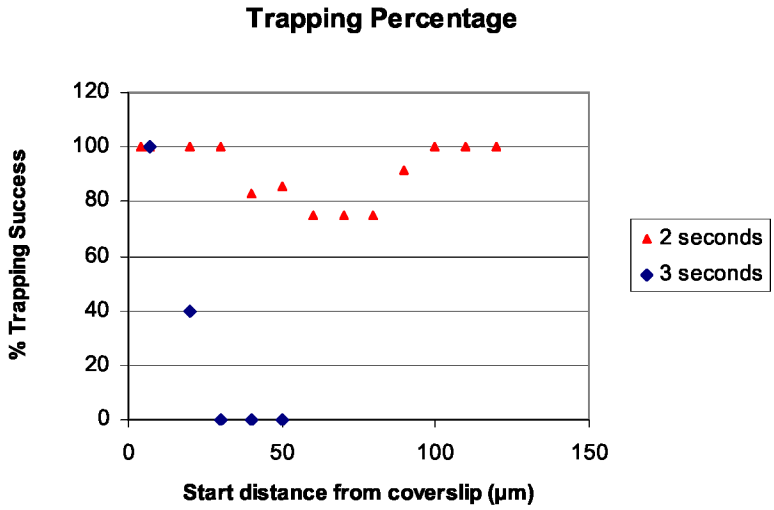

Figure 6.—Plot showing the success rate of retrapping for average times of 2 and 3 sec, starting at varying distances beneath the coverslip.

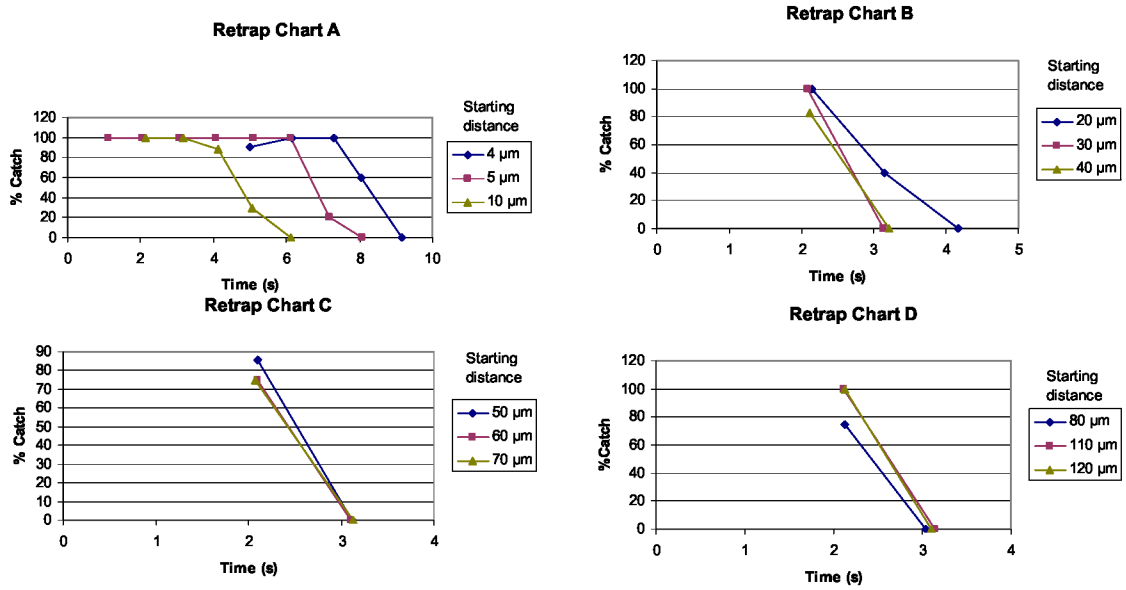

Figure 7.—Plots showing the successful retrap percentages versus falling time from the coverslip for a variety of starting distances beneath the coverslip. The use of lines between data points is employed as a visual aid to help note which data points belong to certain starting distances. The microsphere was lowered 4, 5, and 10 µm before release (A). The microsphere was lowered 20, 30, and 40 µm before release (B). The microsphere was lowered 50, 60, and 70 µm before release (C). The microsphere was lowered 80, 110, and 120 µm before release (D).

In all cases, the success rate of retrapping decreased further from the upper and lower boundaries of the sample chamber. This may be due in part to the sphere moving more slowly in the vicinity of the boundaries, making retrapping more likely. It was also noted while performing the experiments that a microsphere moving near the middle of the sample chamber was much more susceptible to having its trajectory altered by vibrations induced when adjusting the microscope, which also reduces the success rate of retrapping a particle.

Difficulty retrapping microspheres further from the coverslip may also be due in part to the fact that most oil-immersion microscope objective lenses correct for spherical aberration of the trapping beam near the coverslip, rather than deeper into a sample chamber, (Ref. 21) and also may be due to physical boundary conditions that proximity to the coverslip presents to the microsphere. Having fewer spherical

aberrations near the coverslip does not explain why retrapping became easier near the bottom of the sample chamber, but the sphere has an increased proximity to physical boundaries in this region, which may help provide stability to the motion of the sphere.

Conclusion

Timing a falling microsphere for successively longer periods of time reveals that terminal velocity is reached very quickly after releasing a microsphere from an optical trap in the sealed sample chambers. Thus, the terminal velocity of the falling sphere may be considered constant for purposes of computing the distance over which an optical trap can draw in objects, except when the microsphere is less than two sphere diameters from the top of the sample cell. The details of how the sample cell environment affects the falling sphere are not completely understood at this time. There may be some electrostatic forces close to the coverslip, between the coverslip and the microsphere, and it may take some time for the smooth flow of fluid around the falling sphere to set up. These experiments were attempted with a variety of sizes of microsphere, but only the 9.975 μm diameter spheres available to me at that time were found to not contain any residual static charge on the surface of the spheres. It is not possible at this time to measure the trapping length with precision enough to determine weather the trap length favors an apertured, focused, and aberrated (AFA) beam model or a Gaussian beam model. However, it can be stated that in most locations within the sample chamber, this optical trap reaches "downward" to draw microspheres up over a distance of between 6 and 7 μm. It can also be stated that 2 sec appears to be the optimum time needed to retrap a falling microsphere without necessitating moving the optical trap. Moving the optical trap involves moving parts of the microscope which can introduce vibrations in the sample chamber which can also make it difficult to reacquire the microsphere with the trap. Additionally, it appears that when a microsphere is within two diameters from an upper or lower boundary in the sample chamber may not move as quickly as it does near the middle of the chamber, resulting in longer times available for retrapping the same object.

The temperature of the water inside the sample chamber had a noticeable effect on the viscosity of the water. The sample illumination light was found to warm the sample as much as 14 °C during several hours of data accumulation. Future measurements should benefit from tracking the temperature of the sample chamber so as to have a reliable determination of the viscosity of the water in the chamber at the time of data collection. Timing of a falling microsphere may be improved if a beam block and timing device can be precisely connected to lessen uncertainty in time measurements.

It was found that the upper and lower boundaries of the sample chamber influence the time available to retrap a falling object in such a way that it is easier to trap falling microsphere in those areas. Also it was found that it is more difficult to trap a falling microsphere near the middle of the sample chamber. Increased spherical aberration of the optical trap, and having fewer constraints on the motion of the fluid as water molecules slip past the falling sphere may contribute to this difficulty. While retrapping was more difficult near the center of the chamber, greater than 70 percent success rate was achieved.

This will help in predicting how particles can be moved into position when using optical traps as tools for building small devices.

References

1. NASA Fundamental Aeronautics Program, http://www.aeronautics.nasa.gov/fap/index.htm
2. NASA Subsonic Fixed Wing Program, http://www.aeronautics.nasa.gov/fap/subfixed.html#performance
3. Stetter, R., Hesketh, P.J., Hunter, G.W., "Sensors: Engineering Structures and Materials From Micro to Nano," *Interface,* Spring 2006 pp. 66–69.
4. Abid, M.M., Spacecraft Sensors, John Wiley & Sons, 2005.

5. C. Liu, R. Vander Wal, G. Hunter, "Microchemical and Gaseous Sensors Using Carbon Nanotubes and MEMS Fabrication Technology," NASA/TM—2003-212209, April 2003.
6. G. Zhang, B. Guo, J. Chen, "MCo_2O_4 (M=Ni, Cu, Zn) nanotubes: Template synthesis and application in gas sensors," *Sensors and Actuators B,* 114, pp. 402–409, 2006.
7. Y. Liu, H. Yang, Y. Yang, Z. Liu, G. Shen, R. Yu, "Gas sensing properties of tin dioxide coated onto multiwalled carbon nanotubes," *Thin Solid Films,* 497, pp. 355–360, 2006.
8. G.T. Pham, Y. Park, Z. Liang, C. Zhang, B Wang, "Processing and modeling of conductive thermoplastic/carbon nanotube films for strain sensing," *Composites: Part B,* 39, pp. 209–216, 2008.
9. C. Thelander, L. Samuelson, "AFM manipulation of carbon nanotubes: realization of ultra-fine nanoelectrodes" *Nanotechnology,* 13, pp. 108–113, 2002.
10. A.J. Wright, T.A. Wood, M.R. Dickinson, H.F. Gleeson, T. Mullin, "The transverse trapping force of an optical trap: factors affecting its measurement," *Journal of Modern Optics,* 50, pp. 1521–1532, 2003.
11. F. Gittes, C.F. Schmidt, "Interference model for back-focal-plane displacement detection in optical teeezers," *Optics Letters,* 23, pp. 7–9, 1998.
12. L.P. Ghislain, W.W. Webb, "Scanning-force microscope based on an optical trap," *Optics Letters,* 18, pp. 1678–1076, 1993.
13. W. Singer, S. Bernet, N. Hecker, M. Ritsch-Marte, "Three-dimensional force calibration of optical tweezers," *Journal of Modern Optics,* 47, pp. 2921–2931, 2000.
14. L.P. Ghislain, N.A. Siwtz, W.W. Webb "Measurement of small forces using an optical trap," *Review of Scientific Instruments,* 65 pp. 2762–2768, 1994.
15. A. Ashkin, J.M. Dziedzic, J.E. Bjorkjolm, S. Chu, "Observation of a single-beam gradient force optical trap for dielectric particles," *Optics Letters*, 11, pp. 288–290.
16. A. Ashkin, "Acceleration and trapping of particles by radiation pressure," *Physical Review Letters,* 24, pp. 156–159.
17. G. Stokes, "On the effect of the internal friction of fluids on the motion of pendulums," Trans. Camb. Phil. Soc, Vol. IX. (1851) p. [8], 1850.
18. J. Lock, S. Wrbanek, K. Weiland, "Scattering of a tightly focused beam by an optically trapped particle," *Applied Optics,* 45, pp. 3634–3644, 2006.
19. Wright, W.H., Sonek, G.J., Berns, M.W., "Parametric study of the forces on microspheres held by optical tweezers," *Applied Optics,* 99, pp. 1735–1748, 1994.
20. Happel, J., Brenner, H., Low Reynolds Number Hydrodynamics with special applications to particulate media, Kluwer Academic Publishers, 1991.
21. Axner, O., Fällman, E., "Influence of a glass-water interface on the on-axis trapping of micrometer-sized spherical objects by optical tweezers," *Applied Optics,* 42, pp. 3915–3926.

REPORT DOCUMENTATION PAGE		Form Approved OMB No. 0704-0188

1. REPORT DATE *(DD-MM-YYYY)*	2. REPORT TYPE	3. DATES COVERED *(From - To)*
01-05-2009	Technical Memorandum	

4. TITLE AND SUBTITLE
Measurement of Trap Length for an Optical Trap

5a. CONTRACT NUMBER

5b. GRANT NUMBER

5c. PROGRAM ELEMENT NUMBER

6. AUTHOR(S)
Wrbanek, Susan, Y.

5d. PROJECT NUMBER

5e. TASK NUMBER

5f. WORK UNIT NUMBER
WBS 561581.02.08.03.14.03

7. PERFORMING ORGANIZATION NAME(S) AND ADDRESS(ES)
National Aeronautics and Space Administration
John H. Glenn Research Center at Lewis Field
Cleveland, Ohio 44135-3191

8. PERFORMING ORGANIZATION REPORT NUMBER
E-16674

9. SPONSORING/MONITORING AGENCY NAME(S) AND ADDRESS(ES)
National Aeronautics and Space Administration
Washington, DC 20546-0001

10. SPONSORING/MONITORS ACRONYM(S)
NASA

11. SPONSORING/MONITORING REPORT NUMBER
NASA/TM-2009-215508

12. DISTRIBUTION/AVAILABILITY STATEMENT
Unclassified-Unlimited
Subject Category: 74
Available electronically at http://gltrs.grc.nasa.gov
This publication is available from the NASA Center for AeroSpace Information, 301-621-0390

13. SUPPLEMENTARY NOTES

14. ABSTRACT
The trap length along the beam axis for an optical trap formed with an upright, oil-immersion microscope was measured. The goals for this effort were twofold. It was deemed useful to understand the depth to which an optical trap can reach for purposes of developing a tool to assist in the fabrication of miniature devices. Additionally, it was desired to know whether the measured trap length favored one or the other of two competing theories to model an optical trap. The approach was to trap a microsphere of known size and mass and raise it from its initial trap position. The microsphere was then dropped by blocking the laser beam for a pre-determined amount of time. Dropping the microsphere in a free-fall mode from various heights relative to the coverslip provides an estimate of how the trapping length changes with depth in water in a sample chamber on a microscope slide. While it was not possible to measure the trap length with sufficient precision to support any particular theory of optical trap formation, it was possible to find regions where the presence of physical boundaries influenced optical traps, and determine that the trap length, for the apparatus studied, is between 6 and 7 μm. These results allow more precise control using optical micromanipulation to assemble miniature devices by providing information about the distance over which an optical trap is effective.

15. SUBJECT TERMS
Optical tweezers; Nanotechnology; Laser tweezers; Microscopy; Optical microscopes; Video microscopy

16. SECURITY CLASSIFICATION OF:			17. LIMITATION OF ABSTRACT	18. NUMBER OF PAGES	19a. NAME OF RESPONSIBLE PERSON
a. REPORT	b. ABSTRACT	c. THIS PAGE			STI Help Desk (email:help@sti.nasa.gov)
U	U	U	UU	18	19b. TELEPHONE NUMBER *(include area code)* 301-621-0390